A Working Electron Impact Cross Section Set for CHF_3

Mark J. Kushner[a)] and Da Zhang[b)]
University of Illinois
1406 W. Green St
Urbana, IL 61801

Abstract

Trifluoromethane, CHF_3, is used for plasma etching of silicon compounds for microelectronics fabrication, and so there is interest in developing computer models for plasmas sustained in CHF_3. Recent measurements of electron swarm parameters, and electron impact dissociation and ionization cross sections, have provided a sufficient basis to develop a working electron impact cross section set for CHF_3. Such a cross section set is reported here. We found that increased energy losses from dissociative electronic excitation processes were required to reproduce experimental ionization coefficients. The cross sections for attachment are small with there being some uncertainty in their magnitude at low energies. The cross sections were used in a plasma equipment model for an inductively coupled plasma reactor and compared to discharges sustained in C_2F_6. For otherwise identical operating conditions, plasmas sustained in CHF_3 had higher electron and lower negative ion densities.

[a)] Department of Electrical and Computer Engineering. electronic mail: mjk@uiuc.edu

[b)] Department of Materials Science and Engineering. electronic mail: dzhang@uiuc.edu

I. Introduction

Trifluoromethane, CHF_3, is a gas extensively used in the microelectronics industry for etching of silicon compounds. [1-3] As a result, there is great interest in developing reaction mechanisms for gas mixtures containing CHF_3 for use in computer models of plasma processing reactors. Recent reviews and assessments of fundamental data [4,5] and recent measurements of electron swarm data in CHF_3 [6] and Ar/CHF_3 mixtures [7] have provided sufficient background that a working electron impact cross section set for CHF_3 for modeling can be constructed. Morgan has recently discussed compilation of such a cross section set based on swarm measurements and ab-initio calculations.[8] In this paper, the development of a cross section set will be discussed and the derived values will be presented. The cross section set was used in a model of a plasma etching reactor and results for plasma densities will be presented.

II. Development of the CHF_3 Cross Section Set

The current literature on electron impact interactions with CHF_3 is discussed in detail in Refs. 4, 5, and 7. The highlights from those works, which are of particular interest here, are as follows. 1) There is uncertainty in the magnitude of the cross sections for specific branchings of neutral dissociation. 2) There is a factor of two disagreement in total ionization cross section between all measurements and calculations. 3) Attachment for $E/N < 50$ Td (1 Td = 10^{-17} V-cm_2) is weak, with some question as to whether measured attachment rates at low E/N may be a result of impurities. 4) There are relative cross sections available for attachment producing F^- which indicate a resonance near 10 eV. 5) Measurements for total scattering are available. 6) Calculated momentum transfer cross sections are available for a limited range of energies.

As a starting point, the neutral dissociation and partial ionization cross sections of Goto were used without modification. [9] The cross sections were linearly extrapolated to zero at threshold from the lowest energy cross section available. Dissociative attachment was included using the shape of the F^- yield as a function of energy measured by Scheunemann et al.[10] As a first estimate for the momentum transfer cross section, the total scattering cross section recommended by Christophorou and Olthoff [5] was used at energies below 10 eV, mated to calculations of momentum transfer above 10 eV by Natalense et al.[11] Vibrational excitation cross sections were introduced using as threshold energies the values given by Hertzberg for fundamental modes 1-6.[12] Cross sections for nearly degenerate modes were combined yielding three vibrational electron-impact cross sections with thresholds: $\nu 14$, 0.37 eV; $\nu 25$, 0.18 eV and $\nu 36$, 0.13 eV.

These cross sections were used as input to a solution of Boltzmann's equation for the electron energy distribution using a 2-term spherical harmonic expansion.[12] The resulting distributions were then used to compute electron drift velocity and net ionization coefficient [$\alpha_0 = \alpha - \eta$ where α is the ionization coefficient (cm^{-2}) and η the attachment coefficient (cm^{-2})] as a function of E/N (electric field/gas number density). Comparisons were made to the experimental swarm measurements of Urquijo et al.[6]

Initial trials produced positive values of α_0 many times that of the experiment with the transition from negative to positive α_0 at a lower E/N than observed experimentally. Additional inelastic or attachment losses were required to bring computed values of α_0 in line with experiment. The magnitudes of the inelastic vibrational cross sections were constrained by the magnitude of the total scattering cross section, and so it was deemed not appropriate to increase their values to sufficiently to decrease α_0. The magnitude of the attachment cross section is likely to be only on the order of 10^{-19} cm^2 [4] and is constrained by the small values of experimentally measured η at low E/N. Therefore an additional electronic non-ionizing inelastic energy loss was required. This loss was accomplished by increasing the magnitude of the neutral dissociation cross sections since their values are the most uncertain and those reported by Goto are likely too small.[5,14,15] The neutral dissociation cross sections were scaled by values up to 20. Although the appropriate magnitude of α_0 could be obtained, the slope of α_0 vs E/N could not be matched to swarm data without introducing additional energy loss near threshold. The cross section for the 11.0 eV threshold process ($e + CHF_3 \rightarrow CF_3 + H + e$) was therefore enhanced near threshold. The magnitude of the resonant peak in attachment at 10 eV, the scaling factor for the neutral dissociation cross sections and the magnitude of the enhancement were adjusted so that computed values of α_0 matched the experimental zero crossing of α_0 at $\approx$ 65 Td and the magnitude and slope of α_0 at higher E/N. The slope of the momentum transfer cross section and the magnitude of the vibrational cross sections were adjusted to match drift velocities. The low energy foot to the attachment cross section was also increased to provide thermal attachment rates of $3\text{-}4 \times 10^{-14}$ cm^3 s^{-1} [7]. The cross section for dissociation into CF was arbitrarily partitioned into two equal branchings yielding $CF + H + F_2$ and $CF + H + 2F$, an assumption which has no effect on the computed swarm parameters.

III. Cross Sections, Swarm Data and Plasma Parameters

The resulting cross sections and comparisons of computed swarm data to experiments are shown in Figs. 1-3. Representative electron energy distributions are shown in Fig. 4. Complete tabular data of the cross sections can be obtained by request from the author or can be downloaded from the author's website (http://uigelz.ece.uiuc.edu/data). The momentum transfer cross section decreases nearly monotonically with energy with a small enhancement near 1 eV in the vicinity of the vibrational cross sections. The nearly flat portion at 2-7 eV was required to lower the drift velocity in the 10's Td regime while the cross sections from 10-30 eV were constrained by the values from calculations from Natalanse et al.[11] The neutral dissociation cross sections were scaled by a factor of 5 from those reported by Goto.[9]. The resulting values are commensurate with measurements by Motlagh and Moore.[15] The enhanced neutral dissociation cross section has a sharply rising leading edge. The calculated swarm parameters are sensitive to this leading edge, however they are not sensitive to the shape of the cross section at energies > 20 eV.

In general the agreement of calculated swarm parameters with experimental data is good. The greatest uncertainties are in the drift velocity in the 20-40 Td range and in the attachment coefficient ($\alpha_0 < 0$) in the 40-60 Td range. Larger negative values of α_0 ($\approx -5 \times 10^{-19}$ cm^2) are computed than indicated experimentally. To eliminate these negative values of α_0 would require that the cross section for attachment at the 10 eV resonant peak be significantly below 10^{-19} cm^2. In the absence of this electron attachment, it is difficult to reproduce the zero crossing in α_0. Increasing the foot in the attachment cross section produces too much attachment at low E/N at electron energies below 1.8 eV where attachment rates are small if they exist at all.

Representative electron energy distributions (EEDs) are shown in Fig. 4 for swarms in pure CHF_3. The EEDs for E/N < 60 Td are shaped by inelastic energy loss through vibrational excitation. At lower E/N, this loss is dominated by v3,6. At the higher E/N, contributions from v2,5 begin to become important. At E/N = 80 Td, energy loss from the enhanced 11.0 eV neutral dissociation process accounts for about 3% of the energy loss, and the lowest threshold ionization process (15.2 eV) accounts for about 0.1%. These fractions increase to 15% and 1% at

100 Td and are responsible for the cut-off of the EED. The electron temperature (T_e = 2/3 <ε>), shown in Fig. 3a, increases rapidly form 0.1 eV to 2-3 eV for E/N < 100 Td. At E/N > 100 Td, the larger rates of power loss to dissociation and ionization results in the electron temperature saturating in the 4-5 eV range

Using this cross section set, simulations were performed of a low pressure inductively coupled plasma reactor of the type used for plasma etching. The model used is the Hybrid Plasma Equipment Model, described in detail in Ref. 16. A schematic of the reactor is in Ref. 17. The operating conditions are 10 mTorr, 300 sccm and power deposition of 200-650 W, values that were chosen to minimize the fractional dissociation. The reactor volume averaged electron and negative ion densities as a function of power for CHF_3 and C_2F_6 at the same conditions are shown in Fig. 5. In both cases, the electron densities scale nearly linearly with power and are 1-5 x 10^{10} cm^{-3}. The electron energy loss processes for the two molecules are commensurate and so for a given power deposition, the electron densities will be approximately the same, although the electron density for CHF_3 is systematically generally larger than for C_2F_6. The attachment cross sections for C_2F_6, though not large, are larger than for CHF_3. This results in a higher rate of attachment and a larger negative ion density for C_2F_6 compared to CHF_3. These trends agree with measurements of electron density and negative ion density by Hebner and Miller [18] in inductively coupled plasmas for similar conditions.

IV. Concluding Remarks

A working cross section set for CHF_3 has been presented and favorably compared to swarm data. Uncertainties in measurements of attachment rates at low E/N have resulted in some uncertainty in the derived attachment cross section. An enhanced dissociation cross section near threshold was used to match the slope of the ionization coefficient to swarm data. Using these cross sections in a plasma equipment model, we found that negative ion densities are generally higher in C_2F_6 compared to CHF_3.

Acknowledgement: This work was supported by the National Science Foundation (CTS 99-74962), the Semiconductor Research Corporation and AFOSR/DARPA. The author thanks Prof. Urquijo for access to his swarm data prior to publication.

References

1. N. R. Rueger, J.J. Beulens, M. Schaepkens, M. F. Doemling, J. M. Mirza, T. E. F. M. Standearts, and G. S. Oehrlein, J. Vac. Sci. Technol. A **15**, 1881 (1997).
2. R. P. Jayaraman, R. T. McGrath, and G. A. Hebner, J. Vac. Sci. Technol. A **17**, 1545 (1999).
3. K. Takahashi, M. Hori and T. Goto, Jpn. J. Appl. Phys. **33**, 4745 (1994).
4. L. G. Christophorou, J. K. Olthoff and M. V. V. S. Rao, *J. Phys. Chem. Ref. Data* **26**, 1 (1997).
5. L. G. Christophorou and J. K. Olthoff, *J. Phys. Chem. Ref. Data* **28**, 967 (1999).
6. J. de Urquijo, I. Alvarez, and C. Cisneros, Phys. Rev. E **60**, 4990 (1999).
7. Y. Wang, L. G. Christophorou, J. K. Olthoff and J. K. Verbrugge, *Chem. Phys. Lett.* **304**, 303 (1999).
8. W. L. Morgan, 52nd Gaseous Electronics Conference, Norfolk, VA, October 1999.
9. M. Goto, K. Nakamura, H. Toyoda and H. Sugai, *Jpn. J. Appl. Phys. Part 1* **33**, 3602 (1994).
10. H.-U. Scheuenemann, M. Heni, E. Illenberger, and H. Baumgartel, *Ber. Bunsenges. Phys. Chem.* **86**, 321 (1982).
11. A. P. P. Natalense, M. H. F. Bettega, L. G. Ferreira and M. A. P. Lima, *Phys. Rev. A* **59**, 879 (1999).
12. G. Hertzberg, "Molecular Spectra and Molecular Structure, II. Infrared and Raman Spectra of Polyatomic Molecules," (Van Nostrand, New York, 1945).
13. S. D. Rockwood, Phys. Rev. A **8**, 2348 (1973).
14. H. Sugai, H. Toyoda, T. Nakano and M. Goto, Contrib. Plasma Phys. **35**, 415 (1995).
15. S. Motlagh and J. H. Moore, J. Chem. Phys. **109**, 432 (1998).
16. S. Rauf and M. J. Kushner, J. Appl. Phys. **83**, 5087 (1998).

17. D. Zhang and M. J. Kushner, J. Appl. Phys. **87**, 1060 (2000).

18. G. A. Hebner and P. A. Miller, J. Appl. Phys. **87**, 7660 (2000).

Figure Captions

1. Derived electron impact cross sections for CHF_3. a) Momentum transfer, b) vibrational excitation, and c) attachment.
2. Derived electron impact cross sections for CHF_3. a) Neutral dissociation. b) Ionization and electronic excitation. The neutral dissociation cross sections from Goto (Ref. 9) were increased by a factor of 5, and a threshold enhancement was added.. The ionization cross sections from Goto were used without change.
3. Electron swarm data for CHF_3. a) Drift velocity and electron temperature. b) Net ionization coefficient. Agreement of calculated swarm parameters with experiment is generally good, with some overestimation of the drift velocity in the 20-40 Td range.
4. Representative electron energy distributions for swarms in CHF_3 for E/N of 5-200 Td.
5. Reactor averaged electron and negative ion densities for inductively coupled plasmas at 10 mTorr in CHF_3 and C_2F_6.

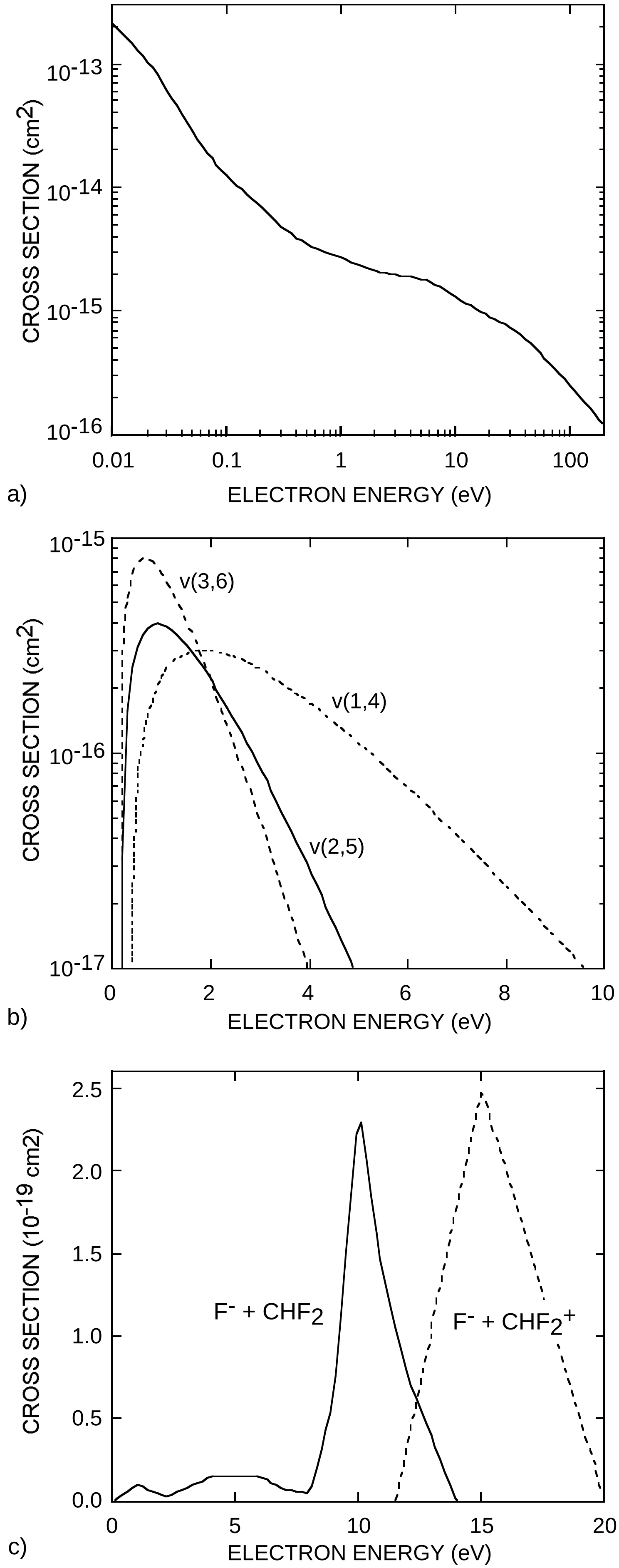

77%

Kushner and Zhang
Figure 1 of 5

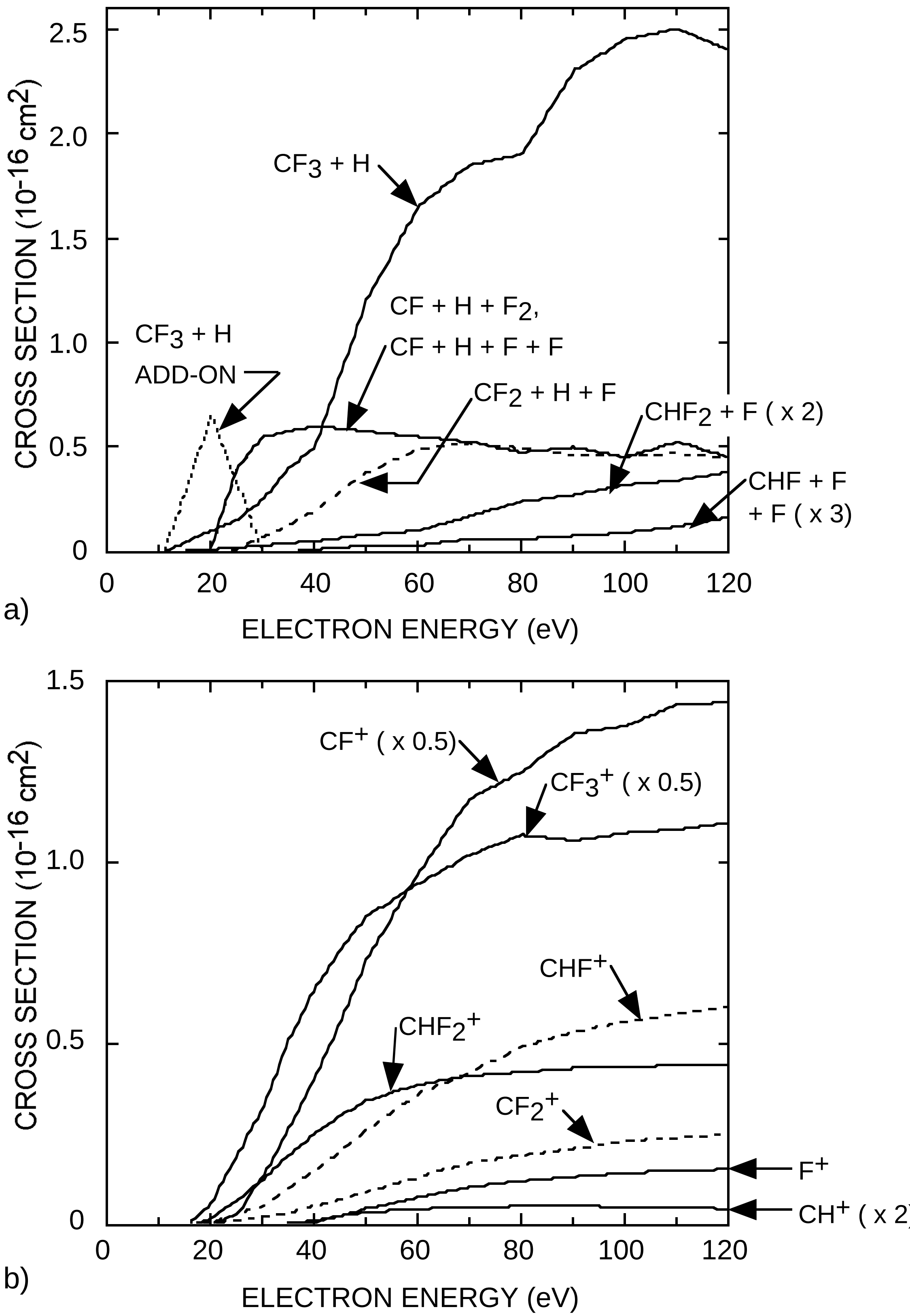

2.5
2.0
1.5
1.0
0.5
0
CROSS SECTION (10^{-16} cm^2)
CF_3 + H
CF + H + F_2,
CF + H + F + F
CF_3 + H
ADD-ON
CF_2 + H + F
CHF_2 + F (x 2)
CHF + F
+ F (x 3)
0
20
40
60
80
100
120
a)
ELECTRON ENERGY (eV)
1.5
1.0
0.5
0
CROSS SECTION (10^{-16} cm^2)
CF^+ (x 0.5)
CF_3^+ (x 0.5)
CHF^+
CHF_2^+
CF_2^+
F^+
CH^+ (x 2)
0
20
40
60
80
100
120
b)
ELECTRON ENERGY (eV)

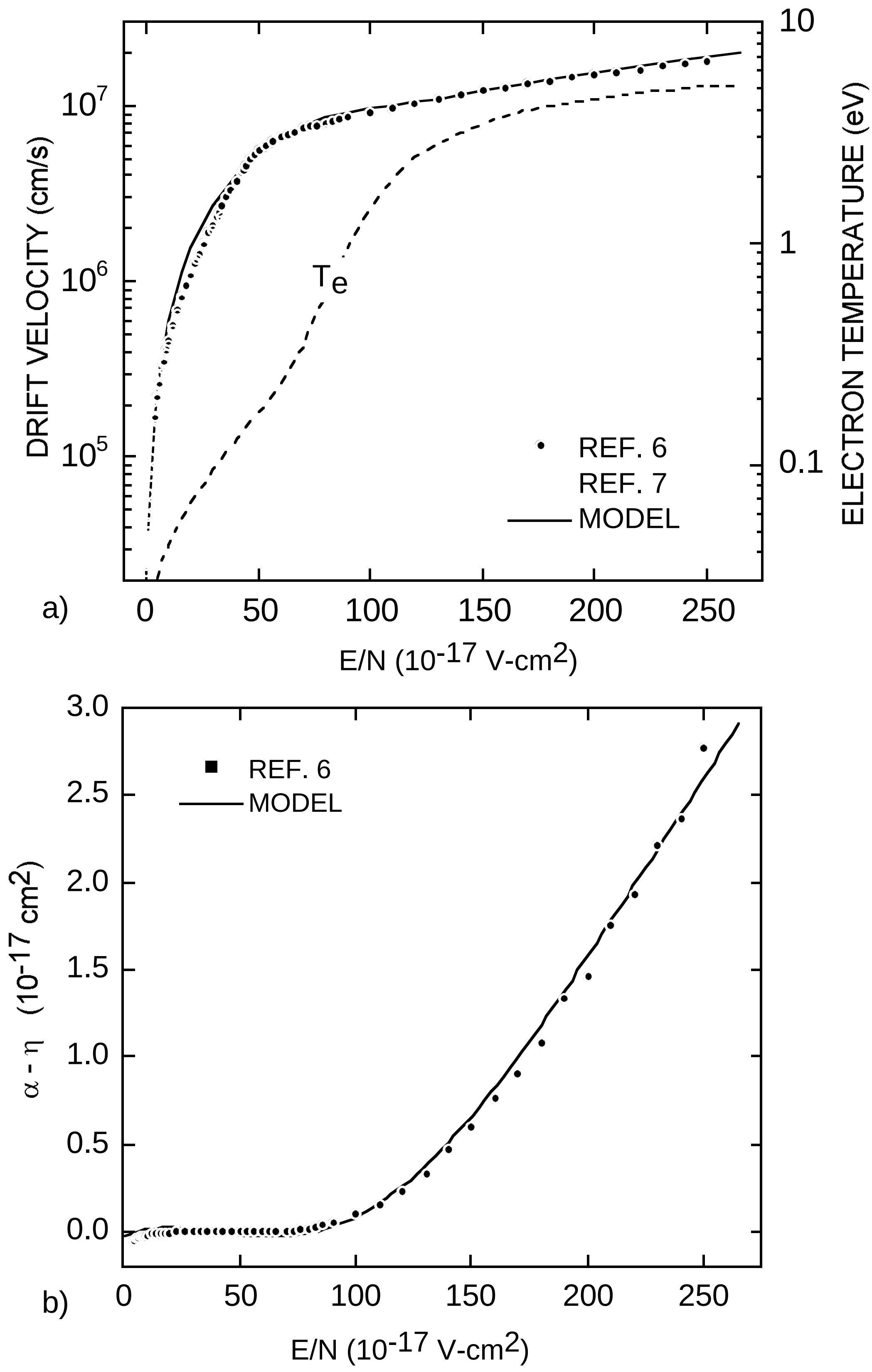

DRIFT VELOCITY (cm/s)
ELECTRON TEMPERATURE (eV)
T_e
REF. 6
REF. 7
MODEL
a)
E/N (10^{-17} V-cm^2)
$\alpha - \eta$ (10^{-17} cm^2)
REF. 6
MODEL
b)
E/N (10^{-17} V-cm^2)

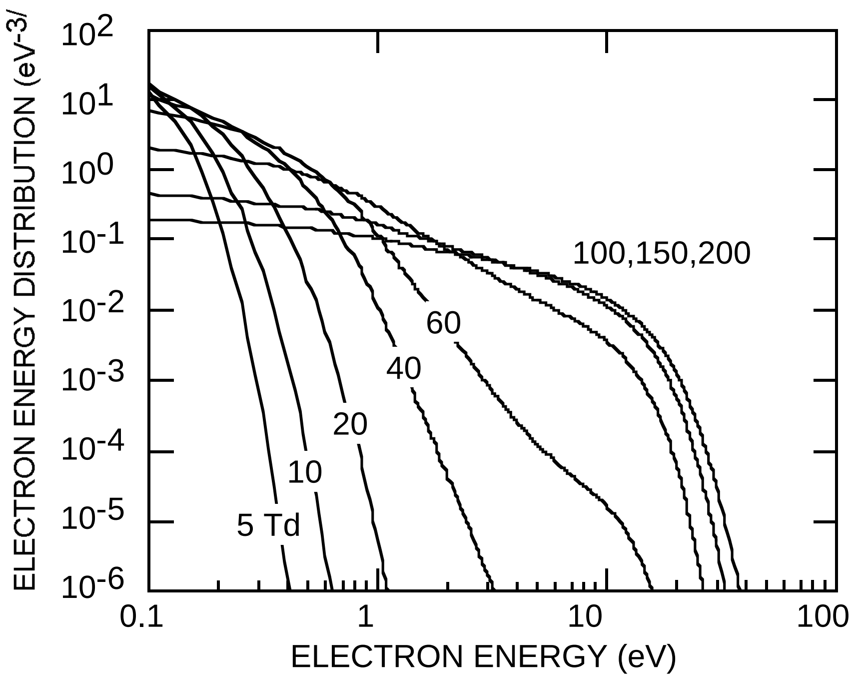
ELECTRON ENERGY DISTRIBUTION (eV-3/
10-6
10-5
10-4
10-3
10-2
10-1
100
101
102
0.1
1
10
100
ELECTRON ENERGY (eV)
100,150,200
60
40
20
10
5 Td

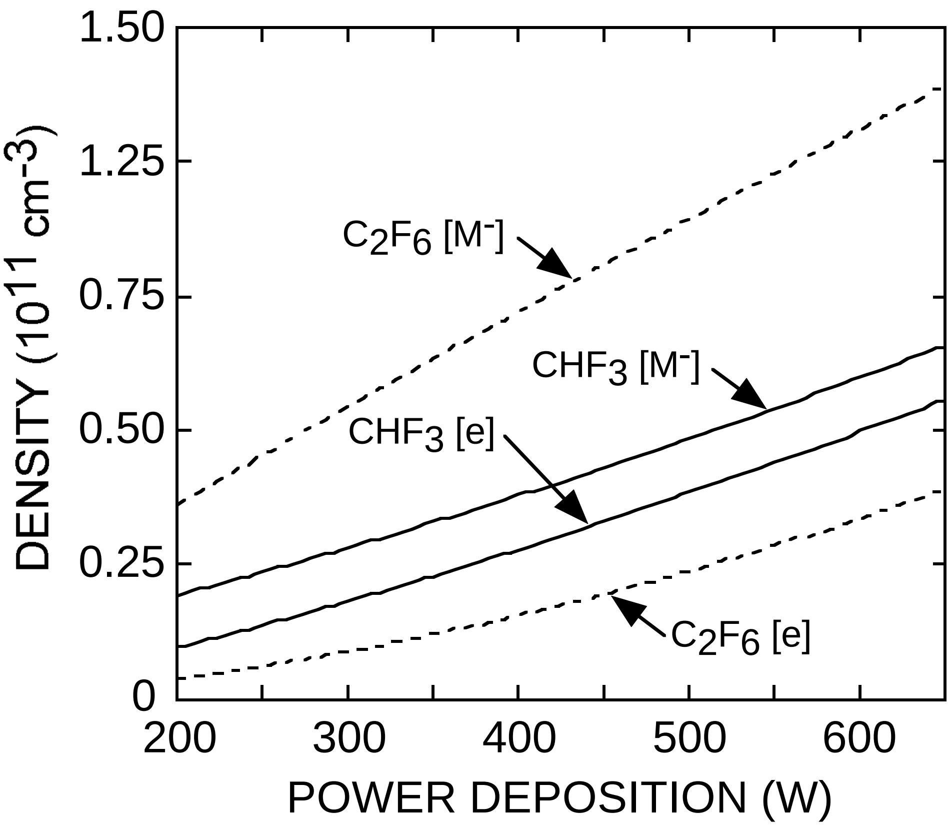
DENSITY (10^{11} cm^{-3})
POWER DEPOSITION (W)
1.50
1.25
0.75
0.50
0.25
0
200
300
400
500
600
C_2F_6 [M^-]
CHF_3 [M^-]
CHF_3 [e]
C_2F_6 [e]